# Integral Equation Solution of Maxwell's Equations from Zero Frequency to Microwave Frequencies

Jun-Sheng Zhao, *Member, IEEE,* and Weng Cho Chew, *Fellow, IEEE*

***Abstract*—We develop a new method to precondition the matrix equation resulting from applying the method of moments (MoM) to the electric field integral equation (EFIE). This preconditioning method is based on first applying the loop-tree or loop-star decomposition of the currents to arrive at a Helmholtz decomposition of the unknown currents. However, the MoM matrix thus obtained still cannot be solved efficiently by iterative solvers due to the large number of iterations required. We propose a permutation of the loop-tree or loop-star currents by a connection matrix, to arrive at a current basis that yields a MoM matrix that can be solved efficiently by iterative solvers. Consequently, dramatic reduction in iteration count has been observed. The various steps can be regarded as a rearrangement of the basis functions to arrive at the MoM matrix. Therefore, they are related to the original MoM matrix by matrix transformation, where the transformation requires the inverse of the connection matrix. We have also developed a fast method to invert the connection matrix so that the complexity of the preconditioning procedure is of $O(N)$ and, hence, can be used in fast solvers such as the low-frequency multilevel fast multipole algorithm (LF-MLFMA). This procedure also makes viable the use of fast solvers such as MLFMA to seek the iterative solutions of Maxwell's equations from zero frequency to microwave frequencies.**

***Index Terms*—Convergence improvement, loop-tree basis, low frequency, surface integral equation.**

## I. Introduction

DUE to the rapidly increasing capability of computers, computational electromagnetics (EMs) is becoming increasingly important. This is partly due to the predictive power of Maxwell's theory as proven over the years—Maxwell's theory can predict the design performances or experimental outcomes if Maxwell's equations are solved correctly. Moreover, Maxwell's theory, which governs the basic principle behind the manipulation of electricity, is also extremely pertinent in many electrical engineering and scientific technologies. Examples of these technologies are radar, remote sensing, geoelectromagnetics, bioelectromagnetics, antennas, wireless communication, optics, high-frequency circuits, etc. Furthermore, Maxwell's theory is valid over a broad range of frequencies spanning static to optics and over a large dynamic range of length scales from subatomic to intergalactic length scales. In view of this, there is always a quest to solve Maxwell's equations accurately from first principles using numerical methods so that increasingly complex structures can be handled.

After the establishment of Maxwell's theory in 1864 [1], [52], the early EMs analyzes were associated with simple shapes such as spheres, cylinders, planes, etc. [2]–[8]. As the scientific and engineering demand for sophistication rose, solutions to more complex geometries were needed. As a result, approximate techniques were developed to solve Maxwell's equations. One can view circuit theory as a reduced form of Maxwell's theory in the low frequency limit where approximate analyzes of many complex geometries have been obtained with astounding success. High-frequency ray theory, diffraction theory, and perturbation theory were developed to provide approximate solutions to Maxwell's theory [9]–[17].[1] With the advent of computer technology in the sixties, numerical methods such as finite-difference method [19], finite-element method [20], and method of moments (MoM) [21], [22] were developed to allow more versatility and accuracy in the solution methods. But for many years, numerical methods could only solve relatively small problems involving a small number of unknowns. However, the recent advances in fast computational algorithms and computer hardware has allowed numerical methods to solve problems of unprecedented sizes involving millions of unknowns [23].

For a closed structure, the surface intergral equation formulations may suffer from the interior resonance problems. The uniqueness of solution of electric field integral equation (EFIE) and magnetic field integral equation (MFIE) is not guaranteed at these interior resonant frequencies [18], [24], [53]. Many remedies have been proposed, such as the combined field integral equation (CFIE) method [25], [26], the extended boundary condition method [27], [28], the combining interior and exterior field expression method [29], the combined-source method [30], and the dual-surface formulation method [31].

However, despite all these advances, there remain many unsolved problems in computational EMs. For example, even though fast Laplace solvers [32], [33] and fast solvers for Helmholtz and related electrodynamic equations exist [34], [35] there does not exist a method that can solve Maxwell's equations rapidly all the way from zero frequency to microwave frequencies. This is an important problem, because there is a pressing need to simulate EM phenomena in circuits and antennas, where the simulated objects or parts can be a tiny fraction of wavelength to a sizable fraction of a wavelength. Therefore, a Maxwell solver should be capable of simulating EM fields corresponding to very long wavelength as well as

Manuscript received September 2, 1999; revised March 10, 2000. This work was supported by AFOSR under MURI Grant F49620-96-1-0025 and a grant from Intel Corp.

The authors are with the Center for Computational Electromagnetics, Electromagnetics Laboratory, Department of Electrical and Computer Engineering, University of Illinois at Urbana-Champaign, Urbana, IL 61801 USA (e-mail: w-chew@uiuc.edu).

Publisher Item Identifier S 0018-926X(00)09376-5.

[1]These references are by no means complete; more references can be found in [18], [53].

short wavelength compared to the size of the simulated object. In this manner, fine details can be simulated accurately, e.g., in circuit components such as inductors and capacitors. In an antenna feed, fine features often dictate the input impedance of the antenna. Such a situation also prevails in geoelectromagnetics [36], where very long wavelength is used to enhance the penetration depth of geophysical probing tools, and the dimensions of the tools and the feature being probed are a small fraction of a wavelength. In addition, electrodynamic phenomena, which are due to the finite wavelength effect, e.g., in high-speed or high-frequency circuits, and resonance behavior of antennas need be simulated accurately.

However, numerical solution of Maxwell's equations at low frequencies is plagued with numerous problems. This is the consequence of the decoupling of electric and magnetic fields in Maxwell's equations right at zero frequency.[2] Also, the electric and magnetic fields become curl free at zero frequency outside the source region

$$\begin{aligned} &\nabla \times \mathbf{E} = 0, \quad \nabla \times \mathbf{H} = \mathbf{J} \\ &\nabla \cdot \epsilon \mathbf{E} = \rho = \lim_{\omega \to 0} \nabla \cdot \mathbf{J}/i\omega, \quad \nabla \cdot \mu \mathbf{H} = 0. \end{aligned} \tag{1}$$

A harmonic time dependence $e^{-i\omega t}$ is assumed here and is applied throughout the paper.

This decoupling of the electrostatic and magnetostatic fields manifests itself in the current by separating itself into a solenoidal (divergence-free) component and a complementary, irrotational (nonsolenoidal or curl-free) component. At zero frequency, the two currents decouple completely: The divergence-free current produces only a magnetic field, while the irrotational current produces only an electric field. Therefore, the current undergoes a natural Helmholtz decomposition.

Notice from the above that the irrotational current requires a divergence that goes to zero with vanishing frequency so as to produce a physically finite charge, *viz.* $\nabla \cdot \mathbf{J} \sim O(\omega), \quad \omega \to 0$. Hence, $\mathbf{J} = \mathbf{J}_{sol} + \mathbf{J}_{irr}$, where the irrotational component, $\mathbf{J}_{irr}$ vanishes with $\omega$ linearly as $\omega \to 0$. Notice that no such frequency scaling is required of the solenoidal component $\mathbf{J}_{sol}$.

Because of the discrepant frequency dependence of the solenoidal and irrotational components of the current when $\omega$ tends to zero, a working numerical method has to include this Helmholtz decomposition and ascribe the requisite frequency dependencies to the solenoidal and irrotational components of the current. This decomposition is achieved by the loop-tree and the loop-star method [37], [38].

In the potential method of solving Maxwell's equation $\mathbf{E} = i\omega\mathbf{A} - \nabla\phi$. The contribution from the charge $\rho$ is related to the scalar potential $\phi$, contribution of the field under a Lorentz gauge, while the contribution from the current $\mathbf{J}$ is related to the vector potential $\mathbf{A}$, contribution of the electric field. At very low frequencies, when the electric field integral equation (EFIE) is solved by the straightforward MoM with the rooftop basis or Rao–Wilton–Glisson (RWG) basis [37], the contribution from the vector potential to the impedance matrix is much smaller than the contribution from the scalar potential due to the lack of consideration of the frequency scaling of the irrotational component of the current as mentioned above. This effect can be gleaned from studying the following integral representation of the electric field:

$$\begin{aligned} \mathbf{E}(\mathbf{r}) = i\omega\mu \int_S g(\mathbf{r}, \mathbf{r}')\mathbf{J}(\mathbf{r}')d\mathbf{r}' \\ - \frac{1}{i\omega\epsilon} \nabla \int_S g(\mathbf{r}, \mathbf{r}')\nabla' \cdot \mathbf{J}(\mathbf{r}')\, d\mathbf{r}'. \end{aligned} \tag{2}$$

Due to the finite machine precision, the contribution from the vector potential (the first term) will be lost during the numerical process when $\omega \to 0$. Furthermore, the scalar potential part in the above integral operator has a null space because of its divergence operator. This makes the impedance matrix nearly singular and difficult to invert at low frequencies [37], [38]. But the vector potential term may be as important as the scalar potential term though it produces an electric field $O(\omega)$ smaller at very low frequencies. However, it generates a nonvanishing magnetic field when $\omega \to 0$. The loss of the contribution from the vector potential makes the solution inaccurate [37], [38]. Physically, this corresponds to the problem separating into an inductive part and a capacitive part. However, the inductive effect and capacitive effect can be equally important at low frequencies such as in an LC tank circuit. Therefore, a correct numerical method needs to preserve the inductive phenomenon in addition to the capacitive phenomenon when the frequency goes to zero.

These problems, as mentioned above, are overcome by introducing the loop-star basis and loop-tree basis [37]–[44]. These bases separate the contributions from the vector potential and the scalar potential in the impedance matrix. In this manner, the contribution from the vector potential will not be swamped by that from the scalar potential after an appropriate frequency normalization. Therefore, the impedance matrix is no longer nearly singular, the physics of the inductive phenomenon and capacitive phenomenon is captured correctly and the solutions are much more accurate.

The use of the loop-star or the loop-tree basis, followed by frequency normalization, only solves the problem of singular matrices partially at very low frequencies. The matrix, however, is still ill-conditioned. If an iterative solver is used, the iteration count is usually very large and may even diverge for some problems.

In many cases, the matrix equation has to be solved by an iterative solver. For example, the only known path to large scale computing involving millions of unknowns is via iterative solvers. Direct inversion methods cannot be used due to the $O(N^2)$ memory and $O(N^3)$ central processing unit (CPU) time requirements. In comparison, the low-frequency multilevel fast multipole algorithm (LF-MLFMA) [45] has a memory requirement of $O(N)$ and the number of floating-point operations per iteration is of $O(N)$. But the LF-MLFMA is based on iterative solvers. Also there are cases where iterative solvers are preferred: for example, when a sweep of frequencies or a sweep of incident wave angles for plane wave excitation is needed, an iterative solver has an advantage because the solution at each step of the sweep is a good initial guess for the next step. Therefore, we cannot avoid the use of iterative

[2]The complete decoupling does not exist in a conductive medium, however, and we will treat this situation in a later paper.

solvers in many cases and the convergence problem of the matrix equation based on the loop-star and loop-tree basis needs to be overcome.

In this paper, we develop a method to transform the matrix equation obtained by the loop-star or loop-tree method. The new impedance matrix thus obtained has a very good spectral property. When the new matrix equation is solved by iterative solvers, it converges much faster than the original one. This transformation of the matrix equation is motivated by noticing that for electrostatic problems, where Laplace's equation is solved, no convergence problem has been observed. Therefore, a connection matrix is developed to rearrange the basis functions associated with the loop-tree or loop-star method so that they reduce to the electrostatic case at zero frequency.

The rearrangement of the basis can be viewed as a preconditioner via a change of basis and, hence, is equivalent to a matrix transformation of the original matrix equation. This transformation of the matrix requires the inverse of the connection matrix. Hence, for the loop-tree basis, we have developed a method to perform the multiplication (action) of the inverses of the connection matrix (or its transpose) with a vector in only $O(N)$ operations, where $N$ is the number of unknowns. Consequently, the total number of floating-point operations for the rearrangement scales as $O(N)$. This makes viable the use of this method together with LF-MLFMA to solve large-scale problems since the computational complexity of LF-MLFMA is of $O(N)$.

A note is in order on the fast multipole algorithm—its form as reported in the literature [23], [34], [35], breaks down at low frequencies as well. However, a frequency renormalized version can be developed that can give reduced computational complexity at low frequencies [45]. Therefore, a fast algorithm for a matrix-vector product now exists all the way from zero frequency to microwave frequencies.

## II. General Equations

In this section, we first give a brief review of the original matrix equation for a system of conducting bodies interconnected by wires based on the loop-star and loop-tree basis. After illustrating the problem with the original equations, we present a method to transform the matrix equation to obtain a good convergence property. Then we discuss a method to perform the multiplication (action) of the inverses of the connection matrix and its transpose with a vector efficiently for the tree basis. The details are shown in the following subsections.

### A. Original Matrix Equation with Loop-Tree Basis

The EFIE of three-dimensional perfectly conducting bodies interconnected by wires can be written as

$$\begin{aligned} i\omega\mu\hat{t}(\mathbf{r})\cdot\int_S g(\mathbf{r},\mathbf{r}')\mathbf{J}(\mathbf{r}')\,d\mathbf{r}' - \frac{1}{i\omega\epsilon}\hat{t}(\mathbf{r}) \\ \cdot\nabla\int_S g(\mathbf{r},\mathbf{r}')\nabla'\cdot\mathbf{J}(\mathbf{r}')\,d\mathbf{r}' \\ = -\hat{t}(\mathbf{r})\cdot\mathbf{E}^{\text{inc}}(\mathbf{r}), \qquad \mathbf{r}\in S \end{aligned} \tag{3}$$

where $\mathbf{E}^{\text{inc}}(\mathbf{r})$ represents the incident electric fields and $\hat{t}(\mathbf{r})$ is an arbitrary tangential unit vector on the surface. Using the loop-tree basis designed for low-frequency problems

$$\mathbf{J}(\mathbf{r}') = \sum_{n=1}^{N_L} I_{Ln}\mathbf{J}_{L_n}(\mathbf{r}') + \sum_{n=1}^{N_C} I_{Cn}\mathbf{J}_{C_n}(\mathbf{r}') \tag{4}$$

where $\mathbf{J}_{L_n}(\mathbf{r}')$ and $\mathbf{J}_{C_n}(\mathbf{r}')$ are, respectively, divergence-free loop basis and nondivergence-free tree basis defined in [37]–[44]. $\mathbf{J}_{L_n}(\mathbf{r}')$ is a surface-loop basis, a wire-loop basis, or a wire-surface-loop basis. $\mathbf{J}_{C_n}(\mathbf{r}')$ is a surface-tree basis, a wire-tree basis, or a wire-surface-junction basis as defined in [46]–[48]. Equation (4) can be rewritten in the matrix form as

$$\mathbf{J}(\mathbf{r}') = \mathbf{J}_L^t(\mathbf{r}')\cdot\mathbf{I}_L + \mathbf{J}_C^t(\mathbf{r}')\cdot\mathbf{I}_C \tag{5}$$

where $\mathbf{J}_L(\mathbf{r}')$, $\mathbf{I}_L$, $\mathbf{J}_C(\mathbf{r}')$, $\mathbf{I}_C$ are column vectors containing $\mathbf{J}_{L_n}(\mathbf{r}')$, $I_{Ln}$, $\mathbf{J}_{C_n}(\mathbf{r}')$, and $I_{Cn}$, respectively.

The first term in (5) is divergence free, but (5) does not represent a complete Helmholtz decomposition because the second term is not curl free. However, as shall be shown, a complete Helmholtz decomposition is not mandatory to solve this problem as long as the second term always has a component in the curl free-space. By substituting (5) into (3), testing with $\mathbf{J}_L(\mathbf{r})$ and $\mathbf{J}_C(\mathbf{r})$, and applying $\nabla\cdot\mathbf{J}_L(\mathbf{r}) = \mathbf{0}$, we have the matrix equation

$$\begin{bmatrix} \overline{\mathbf{Z}}_{LL} & \overline{\mathbf{Z}}_{LC} \\ \overline{\mathbf{Z}}_{CL} & \overline{\mathbf{Z}}_{CC} \end{bmatrix}\cdot\begin{bmatrix} \mathbf{I}_L \\ \mathbf{I}_C \end{bmatrix} = \begin{bmatrix} \mathbf{V}_L \\ \mathbf{V}_C \end{bmatrix} \tag{6}$$

where

$$\begin{aligned} \mathbf{V}_L &= -\langle\mathbf{J}_L(\mathbf{r}),\,\mathbf{E}^{\text{inc}}(\mathbf{r})\rangle \\ \mathbf{V}_C &= -\langle\mathbf{J}_C(\mathbf{r}),\,\mathbf{E}^{\text{inc}}(\mathbf{r})\rangle \\ \overline{\mathbf{Z}}_{LL} &= i\omega\mu\langle\mathbf{J}_L(\mathbf{r}),\,g(\mathbf{r},\,\mathbf{r}'),\,\mathbf{J}_L^t(\mathbf{r}')\rangle \\ \overline{\mathbf{Z}}_{LC} &= i\omega\mu\langle\mathbf{J}_L(\mathbf{r}),\,g(\mathbf{r},\,\mathbf{r}'),\,\mathbf{J}_C^t(\mathbf{r}')\rangle \\ \overline{\mathbf{Z}}_{CL} &= i\omega\mu\langle\mathbf{J}_C(\mathbf{r}),\,g(\mathbf{r},\,\mathbf{r}'),\,\mathbf{J}_L^t(\mathbf{r}')\rangle = \overline{\mathbf{Z}}^t{}_{LC} \\ \overline{\mathbf{Z}}_{CC} &= i\omega\mu\langle\mathbf{J}_C(\mathbf{r}),\,g(\mathbf{r},\,\mathbf{r}'),\,\mathbf{J}_C^t(\mathbf{r}')\rangle \\ &\quad -\frac{i}{\omega\epsilon}\langle\nabla\cdot\mathbf{J}_C(\mathbf{r}),\,g(\mathbf{r},\,\mathbf{r}'),\,\nabla'\cdot\mathbf{J}_C^t(\mathbf{r}')\rangle. \end{aligned}$$

In the above,

$$\langle\mathbf{A}(\mathbf{r}),\,g(\mathbf{r},\,\mathbf{r}'),\,\mathbf{B}^t(\mathbf{r}')\rangle = \int d\mathbf{r}\mathbf{A}(\mathbf{r})\cdot\int d\mathbf{r}'g(\mathbf{r},\,\mathbf{r}')\mathbf{B}^t(\mathbf{r}').$$

Equation (6) is the matrix equation based on the loop-tree basis for solving very-low-frequency problems.

When the frequency is very low, the elements of the impedance matrix, the excitation vector and the results scale with respect to the frequency $\omega$ as follows:

$$\begin{aligned} &\begin{bmatrix} \overline{\mathbf{Z}}_{LL}(O(\omega)) & \overline{\mathbf{Z}}_{LC}(O(\omega)) \\ \overline{\mathbf{Z}}_{CL}(O(\omega)) & \overline{\mathbf{Z}}_{CC}\left(O\left(\frac{1}{\omega}\right)\right) \end{bmatrix}\begin{bmatrix} \mathbf{I}_L(O(1)) \\ \mathbf{I}_C(O(\omega)) \end{bmatrix} \\ &\quad = \begin{bmatrix} \mathbf{V}_L(O(\omega)) \\ \mathbf{V}_C(O(1)) \end{bmatrix} \end{aligned} \tag{7}$$

where the expressions in the brackets are the scaling properties of the matrix elements at very low frequencies or when $\omega\to 0$. The matrix equation in (7) is unbalanced and ill conditioned

when $\omega \to 0$. This imbalance stems from the fact that we use an electric field integral equation, but the inductive part produces dominantly a magnetic field, with a subdominant electric field. Hence, the upper left hand block of the matrix becomes subdominant in an electric field equation. To remedy this, (7) can be frequency normalized in a balanced manner as

$$\begin{bmatrix} \frac{1}{\omega}\mathbf{Z}_{LL}(O(1)) & \mathbf{Z}_{LC}(O(\omega)) \\ \mathbf{Z}_{CL}(O(\omega)) & \omega\mathbf{Z}_{CC}(O(1)) \end{bmatrix} \begin{bmatrix} \mathbf{I}_L(O(1)) \\ \frac{1}{\omega}\mathbf{I}_C(O(1)) \end{bmatrix} = \begin{bmatrix} \frac{1}{\omega}\mathbf{V}_L(O(1)) \\ \mathbf{V}_C(O(1)) \end{bmatrix}. \tag{8}$$

We have also normalized the current associated with the charge $\mathbf{I}_C$, with $\omega^{-1}$ to force it to vanish with vanishing frequency as mandated by the discussion in the introduction. Consequently, $(1/\omega)\mathbf{Z}_{LL}$, $\omega\mathbf{Z}_{CC}$, $(1/\omega)\mathbf{V}_L$ and $\mathbf{V}_C$ remain finite, $\mathbf{Z}_{LC} = \mathbf{Z}_{CL}^t \to 0$ when $\omega \to 0$.

It can be seen from (6) that the contribution from the vector potential has been uplifted and hence preserved because it is separated from the contribution from the scalar potential and boosted at low frequencies. Consequently, low-frequency breakdown does not appear in the numerical computation. Therefore, the frequency-normalized impedance matrix based on the loop-tree basis is no longer nearly singular and the matrix equation can be solved by direct inversion methods without any problem.

But when the matrix equation is solved by iterative solvers, the iteration count is usually very large. As discussed in the introduction, the iterative solvers are the preferred method for many cases. Therefore, it is imperative that we improve the spectral property of the impedance matrix. To this end, a method is presented in the next section.

### *B. Impedance Matrix Transformation by Basis Rearrangement*

To study the spectral property of the impedance matrix in (8) when $\omega \to 0$, we ignore the off-diagonal blocks to simplify the discussion because they are smaller than the diagonal blocks. Then the problem can be divided into two parts: the electrostatic part and the magnetostatic part, which can be solved independently of each other. The magnetostatic part ($\mathbf{Z}_{LL}$) converges very fast, but the electrostatic part ($\mathbf{Z}_{CC}$) converges very slowly. As we know, the matrix equation for electrostatic problem based on pulse basis converges rapidly. That means the charge basis arising from the divergence of the current basis is the main culprit for the matrix ill conditioning. We can transform the matrix equation so that the resultant matrix reduces to that based on the pulse basis in the static limit. The electrostatic part needs to be transformed by basis rearrangement.

Expanding the surface charge densities in terms of the pulse basis set, we have

$$\rho(\mathbf{r}) = \sum_{n=1}^{N_P} Q_n P_n(\mathbf{r}). \tag{9}$$

For a charge neutral system, we must have

$$\int_S \rho(\mathbf{r})\, dS = \sum_{n=1}^{N_P} Q_n \int_{S_n} P_n(\mathbf{r})\, dS = 0. \tag{10}$$

Then

$$\begin{aligned} Q_{N_P} &= -\sum_{n=1}^{N_P-1} \frac{\int_{S_n} P_n(\mathbf{r})\, dS}{\int_{S_{N_P}} P_{N_P}(\mathbf{r})\, dS} Q_n \\ &= -\sum_{n=1}^{N_P-1} g_{nN_P} Q_n \end{aligned} \tag{11}$$

where

$$g_{nN_P} = \frac{\int_{S_n} P_n(\mathbf{r})\, dS}{\int_{S_{N_P}} P_{N_P}(\mathbf{r})\, dS}. \tag{12}$$

Substituting (11) into (9) we have

$$\begin{aligned} \rho(\mathbf{r}) &= \sum_{n=1}^{N_P} Q_n P_n(\mathbf{r}) \\ &= \sum_{n=1}^{N_P-1} \left[P_n(\mathbf{r}) - g_{nN_P} P_{N_P}(\mathbf{r})\right] Q_n \\ &= \mathbf{N}^t(\mathbf{r}) \cdot \mathbf{Q} \end{aligned} \tag{13}$$

where $\mathbf{N}(\mathbf{r})$ and $\mathbf{Q}$ are vectors of length $N_P - 1$ and

$$[\mathbf{N}(\mathbf{r})]_n = P_n(\mathbf{r}) - g_{nN_P} P_{N_P}(\mathbf{r}) \qquad n = 1, 2, \ldots, N_P - 1 \tag{14}$$

$$[\mathbf{Q}(\mathbf{r})]_n = Q_n \qquad n = 1, 2, \ldots, N_P - 1. \tag{15}$$

From the current continuity condition, we have

$$\nabla \cdot \mathbf{J}(\mathbf{r}) = i\omega\rho(\mathbf{r}) \tag{16}$$

where $\mathbf{J}$ and $\rho$ here are surface current and surface charge densities, respectively. After using (5) and (13) in (16) and applying $\nabla \cdot \mathbf{J}_L(\mathbf{r}) = \mathbf{0}$, we have

$$\nabla \cdot \mathbf{J}_C^t(\mathbf{r}) \cdot \mathbf{I}_C = i\omega \mathbf{N}^t(\mathbf{r}) \cdot \mathbf{Q}. \tag{17}$$

Taking the inner product with $\mathbf{P}(\mathbf{r})$, we have

$$\langle \mathbf{P}(\mathbf{r}), \nabla \cdot \mathbf{J}_C^t(\mathbf{r}) \rangle \cdot \mathbf{I}_C = i\omega \langle \mathbf{P}(\mathbf{r}), \mathbf{N}^t(\mathbf{r}) \rangle \cdot \mathbf{Q} \tag{18}$$

where $\mathbf{P}(\mathbf{r})$ is a vector of length $N_P - 1$ such that

$$[\mathbf{P}(\mathbf{r})]_n = P_n(\mathbf{r}), \qquad n = 1, 2, \ldots, N_P - 1. \tag{19}$$

In this manner, $\langle \mathbf{P}(\mathbf{r}), \mathbf{N}^t(\mathbf{r}) \rangle$ is a diagonal matrix and we can rewrite (18) as

$$\mathbf{K} \cdot \mathbf{I}_C = i\omega \mathbf{Q} \tag{20}$$

where $\mathbf{K}$ is a square matrix.

Alternatively, we can test (17) with $\mathbf{N}(\mathbf{r})$ to obtain

$$\langle \mathbf{N}(\mathbf{r}), \nabla \cdot \mathbf{J}_C^t(\mathbf{r}) \rangle \cdot \mathbf{I}_C = i\omega \langle \mathbf{N}(\mathbf{r}), \mathbf{N}^t(\mathbf{r}) \rangle \cdot \mathbf{Q}. \tag{21}$$

In this case, $\langle \mathbf{N}(\mathbf{r}), \mathbf{N}^t(\mathbf{r}) \rangle$ is nondiagonal and we can rewrite the above as

$$\mathbf{K}' \cdot \mathbf{I}_C = i\omega \mathbf{Q}' \tag{22}$$

where

$$\mathbf{K}' = \langle \mathbf{N}(\mathbf{r}), \nabla \cdot \mathbf{J}_C^t(\mathbf{r}) \rangle \tag{23}$$

$$\mathbf{Q}' = \langle \mathbf{N}(\mathbf{r}), \mathbf{N}^t(\mathbf{r}) \rangle \cdot \mathbf{Q}. \tag{24}$$

But the $\mathbf{Q}'$ above does not connect directly to the static problem.

Equations (20) and (22) also imply that $\mathbf{I}_C$ has to scale as $\omega$ when $\omega \to 0$, as is required in the discussion in the introduction. By using (20) in (6), we have

$$\begin{bmatrix} \mathbf{L}_{LL} & i\omega \mathbf{L}_{LC} \\ i\omega \mathbf{L}_{CL} & \mathbf{C}_{CC}^{-1} \end{bmatrix} \begin{bmatrix} \mathbf{I}_L \\ \mathbf{Q} \end{bmatrix} = \begin{bmatrix} \frac{1}{i\omega} \mathbf{V}_L \\ \mathbf{K}^{t^{-1}} \cdot \mathbf{V}_C \end{bmatrix} \tag{25}$$

where

$$\begin{aligned} \mathbf{L}_{LL} &= \frac{1}{i\omega} \mathbf{Z}_{LL} \\ \mathbf{L}_{LC} &= \frac{1}{i\omega} \mathbf{Z}_{LC} \cdot \mathbf{K}^{-1}, \\ \mathbf{L}_{CL} &= \frac{1}{i\omega} \mathbf{K}^{t^{-1}} \cdot \mathbf{Z}_{CL} = \mathbf{L}_{LC}^t \\ \mathbf{C}_{CC}^{-1} &= i\omega \mathbf{K}^{t^{-1}} \cdot \mathbf{Z}_{CC} \cdot \mathbf{K}^{-1} \end{aligned}$$

the $\mathbf{L}_{LL}$ is the self-inductance matrix of the loop basis, $\mathbf{L}_{LC}$ is the mutual inductance matrix between loop and nondivergence-free bases and $\mathbf{C}_{CC}$ is the self capacitance matrix of the nondivergence-free basis. Equation (25) has the same form as the equation for circuit problems [49].

After this matrix transformation, the $\mathbf{C}_{CC}^{-1}$ block of the matrix equation in (25) is exactly the same matrix equation as for the electrostatic case based on the pulse basis. The new form of the matrix equation is well balanced in scaling with respect to $\omega$. The scaling of the matrix is

$$\begin{bmatrix} \mathbf{L}_{LL}(O(1)) & i\omega \mathbf{L}_{LC}(O(\omega)) \\ i\omega \mathbf{L}_{CL}(O(\omega)) & \mathbf{C}_{CC}^{-1}(O(1)) \end{bmatrix} \begin{bmatrix} \mathbf{I}_L(O(1)) \\ \mathbf{Q}(O(1)) \end{bmatrix} = \begin{bmatrix} \frac{1}{i\omega} \mathbf{V}_L(O(1)) \\ \mathbf{K}^{t^{-1}} \cdot \mathbf{V}_C(O(1)) \end{bmatrix}. \tag{26}$$

When applying (25), we should further normalize the matrix equation so that the diagonal elements of the impedance matrix have almost the same order of value. Equation (25) can be further normalized as

$$\begin{bmatrix} \frac{4}{i\omega\mu} \mathbf{Z}_{LL} & \frac{4}{\mu} \mathbf{Z}_{LC} \cdot \mathbf{K}^{-1} \\ \epsilon \mathbf{K}^{t^{-1}} \cdot \mathbf{Z}_{CL} & i\omega\epsilon \mathbf{K}^{t^{-1}} \cdot \mathbf{Z}_{CC} \cdot \mathbf{K}^{-1} \end{bmatrix} \begin{bmatrix} \mathbf{I}_L \\ \mathbf{Q} \end{bmatrix} = \begin{bmatrix} \frac{4}{i\omega\mu} \mathbf{V}_L \\ \epsilon \mathbf{K}^{t^{-1}} \cdot \mathbf{V}_C \end{bmatrix} \tag{27}$$

or rewritten as

$$\begin{bmatrix} \overline{I} & \overline{0} \\ \overline{0} & \mathbf{K}^{t-1} \end{bmatrix} \begin{bmatrix} \frac{4}{i\omega\mu} \mathbf{Z}_{LL} & \frac{4}{\mu} \mathbf{Z}_{LC} \\ \epsilon \mathbf{Z}_{CL} & i\omega\epsilon \mathbf{Z}_{CC} \end{bmatrix} \begin{bmatrix} \mathbf{I}_L \\ \mathbf{K}^{-1} \cdot \mathbf{Q} \end{bmatrix} = \begin{bmatrix} \frac{4}{i\omega\mu} V_L \\ \epsilon \mathbf{K}^{t^{-1}} V_C \end{bmatrix}. \tag{28}$$

As shall be shown later, the transformed matrix has a good spectral property and the matrix equation converges very rapidly.

For the loop-star basis, we use the same technique to transform the matrix equation and give the same form of the representation. The transformed impedance matrices for the loop-star and the loop-tree bases are the same and have the same spectral property.

### C. Inverting the Connection Matrix with $O(N)$ Operations

In implementing the matrix transformation as shown in (28), we need to perform the multiplications (actions) of inverses of the connection matrix and its transpose with a vector. The number of floating-point operations is $O(N^3)$ for a direct inversion method and $O(N^2)$ for an iterative method. Because the complexity of the LF-MLFMA is $O(N)$, the complexity of these multiplications should be no worse than $O(N)$. Luckily, we can perform these multiplications with $O(N)$ floating-point operations for the loop-tree basis. For the loop-star basis, they can always be rearranged into a loop-tree basis by some connection matrix and apply the same algorithm thereafter. We describe the algorithm for the loop-tree basis below.

We rearrange the current basis and the pulse charge basis in a specific order and partition the connection matrix $\mathbf{K}$ into four parts as

$$i\omega \begin{bmatrix} \mathbf{Q}_1 \\ \mathbf{Q}_2 \end{bmatrix} = \mathbf{K} \cdot \begin{bmatrix} \mathbf{I}_{C_1} \\ \mathbf{I}_{C_2} \end{bmatrix} = \begin{bmatrix} \mathbf{A}_1 & \mathbf{B}_1 \\ \mathbf{A}_2 & \mathbf{B}_2 \end{bmatrix} \cdot \begin{bmatrix} \mathbf{I}_{C_1} \\ \mathbf{I}_{C_2} \end{bmatrix} \tag{29}$$

where $\mathbf{I}_{C_2}$ contains the expansion coefficients of all the junction bases and $\mathbf{I}_{C_1}$ contains the expansion coefficients of the rest of the nondivergence-free current bases. $\mathbf{Q}_2$ has the same dimension as $\mathbf{I}_{C_2}$. After this matrix partitioning, the inverse of the connection matrix can be represented as [50], as shown in (30) at the bottom of the next page, where

$$\overline{\mathbf{D}}_2 = \overline{\mathbf{B}}_2 - \overline{\mathbf{A}}_2 \cdot \overline{\mathbf{A}}_1^{-1} \cdot \overline{\mathbf{B}}_1 \tag{31}$$

is a small matrix.

To calculate the multiplication (action) of $\overline{\mathbf{K}}^{-1}$ with a vector, we need first to calculate the following:

$$\mathbf{x}_1 = \overline{\mathbf{A}}_1^{-1} \cdot \mathbf{y}_1 \tag{32}$$

where $\mathbf{y}_1$ is a vector. Equation (32) gives the solution of the following matrix equation:

$$\overline{\mathbf{A}}_1 \cdot \mathbf{x}_1 = \mathbf{y}_1. \tag{33}$$

The matrix partitioning method can also be applied to calculate the inverse of the transpose of the connection matrix. Similarly, when we calculate the multiplication (action) of $\overline{\mathbf{K}}^{t^{-1}}$

with a vector, we need to calculate the solution of the following matrix equation:

$$\overline{\mathbf{A}}_1^{\,t} \cdot \mathbf{x}_1 = \mathbf{y}_1. \tag{34}$$

To avoid all zero elements in one column of $\overline{\mathbf{A}}_1$, $\mathbf{Q}_2$ does not include all the pulse bases associated with one current basis function. If we study $\overline{\mathbf{A}}_1$ carefully, we find that (33) and (34) can be solved recursively with one or several elements which can be obtained directly for any arbitrary structure if $\mathbf{Q}_2$ includes at least one pulse basis for each surface and each wire part except the part that has the removed pulse basis. The number of floating-point operations to solve (33) and (34) recursively is obviously $O(N)$. The matrix $\overline{\mathbf{A}}_1$ is very sparse. It has a maximum of 3 nonzero elements in one row or one column. Therefore, the memory requirement to store the nonzero elements in $\overline{\mathbf{A}}_1$ is $O(N)$. Because the memory requirements for the rest of the matrices and the number of floating-point operations for the rest of the operations in the matrix partitions are all $O(N)$, the total memory requirements, and the number of floating-point operations for performing the multiplication of the inverse of the connection matrix with a vector and the multiplication of the inverse of the transpose of the connection matrix with a vector are all $O(N)$.

If we use the basis rearrangement (22), the techniques described above can also be applied. In this case, $\mathbf{I}_{C_2}$ contains the expansion coefficients of the junction bases and the bases that overlap the pulse basis set that has been removed, $\mathbf{Q}_2$ should satisfy the following rules: 1) it includes at least one pulse basis function for each surface and each wire part and 2) if the pulse basis function which is removed by charge neutrality is not at the end of a wire or a chain of tree basis, $\mathbf{Q}_2$ must include at least one pulse basis on each side of the removed pulse basis.

## III. Excitation Vector of the Loop Basis

Usually the excitation vector for the loop basis is calculated by

$$V_n^L = -\langle \mathbf{J}_n^L(\mathbf{r}),\, \mathbf{E}^{\text{inc}}(\mathbf{r})\rangle. \tag{35}$$

The evaluation of $V^L$ by (35) over a loop may result in substantial cancellation of the electric field vector and a subsequent loss of precision when the loop dimension is very small compared to the wavelength. A method to solve this problem for the magnetostatic problem was presented in [42] and was applied to the low-frequency problem of EFIE [43], [44]. As shown in Fig. 1, the loop basis can be represented as

$$\mathbf{J}_n^L(\mathbf{r}) = \sum_i \mathbf{J}_{ni}^L(\mathbf{r}) = \sum_i \hat{n}_i \times \nabla_S \Psi_i(\mathbf{r}) \tag{36}$$

where

$$\hat{n}_i = \frac{\mathbf{r}_{eb} \times \mathbf{r}_{bd}}{|\mathbf{r}_{eb} \times \mathbf{r}_{bd}|}$$
$$\Psi_i = 1 + \frac{1}{2A_i}\boldsymbol{\rho} \cdot (\mathbf{r}_{eb} \times \hat{n}_i)$$

and $A_i$ is the area of the triangle. Equation (35) can be rewritten as

$$\begin{aligned} V_n^L &= -\langle \mathbf{J}_n^L(\mathbf{r}),\, \mathbf{E}^{\text{inc}}(\mathbf{r})\rangle \\ &= -\sum_i \int \mathbf{J}_{ni}^L(\mathbf{r}) \cdot \mathbf{E}^{\text{inc}}(\mathbf{r})\, dS \\ &= -\sum_i \int \mathbf{E}^{\text{inc}} \cdot (\hat{n}_i \times \nabla_S \Psi_i(\mathbf{r}))\, dS \\ &= \sum_i \int \Psi_i(\mathbf{r}) \hat{n}_i \cdot \nabla \times \mathbf{E}^{\text{inc}}(\mathbf{r})\, dS \\ &= i\omega\mu \sum_i \int \Psi_i(\mathbf{r}) \hat{n}_i \cdot \mathbf{H}^{\text{inc}}(\mathbf{r})\, dS. \end{aligned} \tag{37}$$

There is no cancellation in (37) in the numerical computation. If the incident wave is a plane wave and is represented as $\mathbf{E}^{\text{inc}}(\mathbf{r}) = \mathbf{E}_0 e^{i\mathbf{k}\cdot\mathbf{r}}$, (37) becomes

$$\begin{aligned} V_n^L &= i\omega\mu \sum_i \int \Psi_i(\mathbf{r}) \hat{n}_i \cdot \left(\frac{1}{\eta}\, \hat{k} \times \mathbf{E}^{\text{inc}}(\mathbf{r})\right) dS \\ &= ik \sum_i \int \Psi_i(\mathbf{r}) (\hat{n}_i \times \hat{k}) \cdot \mathbf{E}^{\text{inc}}(\mathbf{r})\, dS. \end{aligned} \tag{38}$$

Alternatively, one can write $\mathbf{E}^{\text{inc}} = i\omega\mathbf{A}^{\text{inc}} - \nabla\phi^{\text{inc}}$, and notice that the scalar potential term in $\mathbf{E}^{\text{inc}}$ contributes to zero in (35).

## IV. Numerical Results

Figs. 2–5 show distributions of eigenvalues in the complex plane for various cases. All eigenvalues are for diagonally preconditioned impedance matrices. The test objects are either an isolated conducting sphere or two conducting spheres connected by a wire. The radius of the sphere is 0.2 m and the length of the wire is 0.5 m. The radius of the wire is 5 mm. The surface of the sphere is discretized by 72 triangular facets, and the wire is discretized by 6 segments.

Fig. 2 shows the distribution of eigenvalues for the RWG basis at a high frequency of 300 MHz and at a very low frequency of 1 KHz. There is a zero eigenvalue at the very-low-frequency case, which causes the matrix equation to be singular due to the divergence operator in the scalar potential term. Therefore, the RWG basis cannot be used at very low frequencies.

Fig. 3 shows the distribution of eigenvalues for loop-tree and the loop-star bases when the frequency is 1 KHz. The eigenvalue at the origin is removed but there is still a cluster of eigenvalues

$$\overline{\mathbf{K}}^{-1} = \begin{bmatrix} \overline{\mathbf{A}}_1^{-1} + \overline{\mathbf{A}}_1^{-1} \cdot \overline{\mathbf{B}}_1 \cdot \overline{\mathbf{D}}_2^{-1} \cdot \overline{\mathbf{A}}_2 \cdot \overline{\mathbf{A}}_1^{-1} & -\overline{\mathbf{A}}_1^{-1} \cdot \overline{\mathbf{B}}_1 \cdot \overline{\mathbf{D}}_2^{-1} \\ -\overline{\mathbf{D}}_2^{-1} \cdot \overline{\mathbf{A}}_2 \cdot \overline{\mathbf{A}}_1^{-1} & \overline{\mathbf{D}}_2^{-1} \end{bmatrix} \tag{30}$$

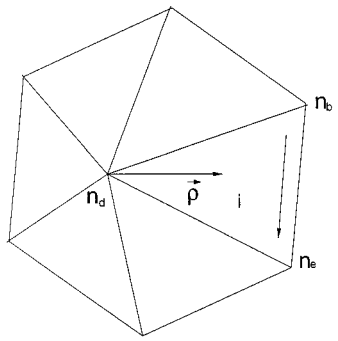


Fig. 1. A loop basis.

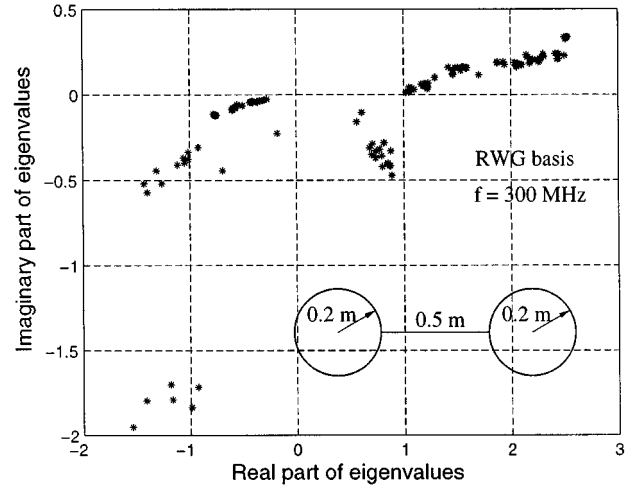


(a)

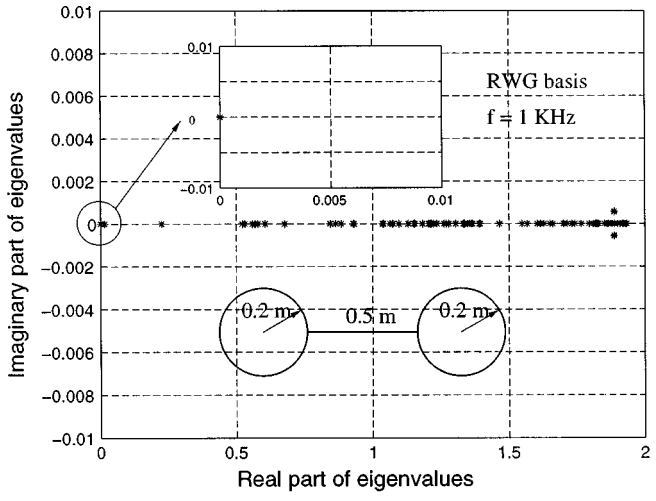


(b)

Fig. 2. The distribution of eigenvalues in the complex plane for RWG basis at various frequencies. (a) Frequency is 300 MHz. (b) Frequency is 1 KHz. Note the existence of a zero eigenvalue at the origin.

near the origin. Hence, the matrix equation from the loop-tree or loop-star basis is still nearly singular. The iteration number is very large when it is solved by an iterative solver.

Fig. 4 shows the distribution of eigenvalues for the loop-tree basis with and without basis rearrangement at a very low frequency of 1 KHz. The basis rearrangement moves the

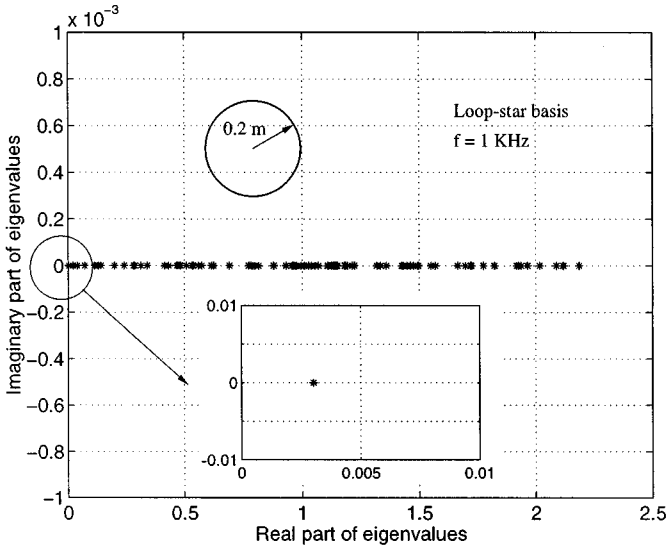


(a)

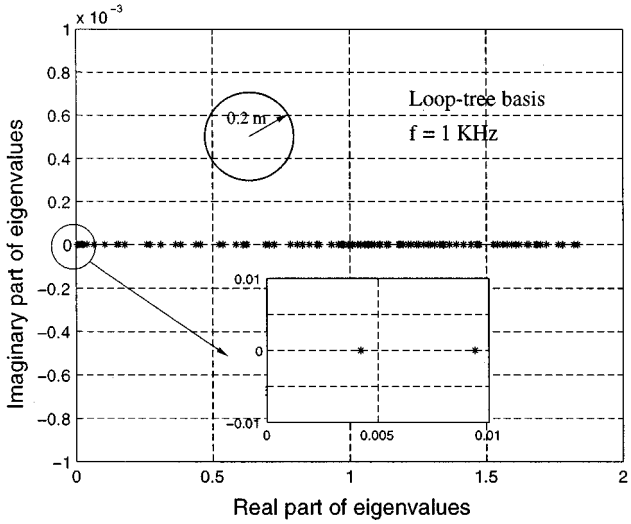


(b)

Fig. 3. The distribution of eigenvalues in the complex plane for (a) loop-star basis and (b) loop-tree basis. The frequency = 1 kHz. A magnification around the origin indicates that the zero eigenvalue has been displaced from the origin.

eigenvalues of the quasi-electrostatic part ($\mathbf{Z}_{CC}$) away from the origin and makes them almost the same as the static case. The quasi-electrostatic part ($\mathbf{Z}_{CC}$) alone with basis rearrangement converges very fast. Because the quasi-magnetostatic part ($\mathbf{Z}_{LL}$) also converges fast and off diagonal blocks ($\mathbf{Z}_{LC}$ and $\mathbf{Z}_{CL}$) are much smaller than diagonal blocks ($\mathbf{Z}_{LL}$ and $\mathbf{Z}_{CC}$), the basis rearrangement makes the transformed matrix equation converge much faster than the original one.

Fig. 5 shows the distribution of eigenvalues for the loop-tree basis with and without basis rearrangement at a high frequency of 300 MHz. Unlike the RWG basis with no eigenvalues near the origin, there is an eigenvalue cluster near the origin for the original loop-tree basis. Therefore, the basis rearrangement is detrimental to the spectral property of the impedance matrix at high frequencies. In addition, the loop-tree basis needs more matrix filling time than the RWG basis. Therefore, we switch over to using the RWG basis when frequency gets high.

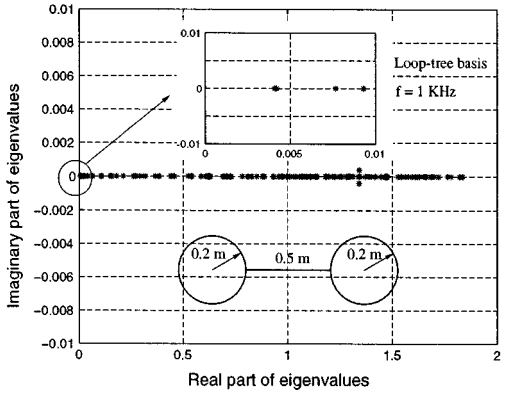


(a)

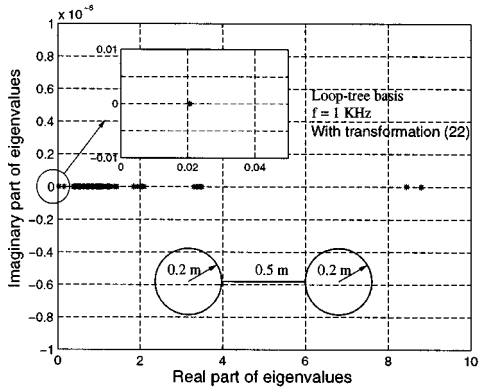


(b)

Fig. 4. The distribution of eigenvalues for loop-tree basis in the complex plane at a low frequency of 1 kHz. (a) Without basis rearrangement. (b) With basis rearrangement (22). (c) With basis rearrangement (20). Note the different scales of the figures. Magnification of the origin shows that rearrangement further removes the eigenvalues from the origin.

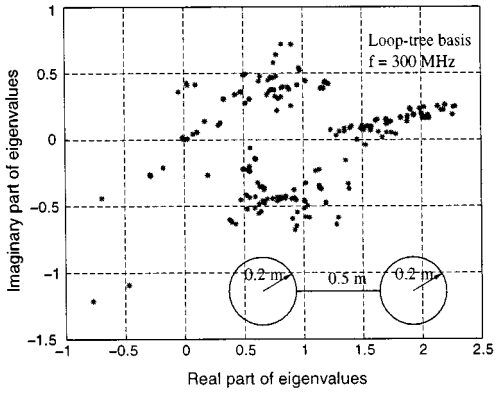


(a)

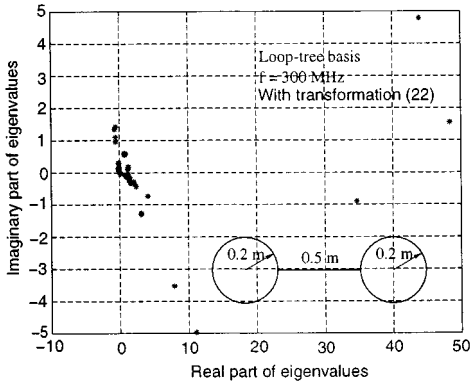


(b)

Fig. 5. The distribution of eigenvalues in the complex plane for loop-tree basis at a high frequency of 300 MHz. (a) Without matrix rearrangement. (b) With matrix rearrangement (22). (c) With matrix rearrangement (20).

Figs. 6 and 7 show the number of iterations used for different forms of matrix equations. To give a fair comparison, the diagonal preconditioning is applied to all cases. The test object for Fig. 6 is a conducting sphere whose radius is 1 m. The sphere is illuminated by a plane wave at a frequency of 1 KHz. The transformed matrix equation uses about 1/10 of the iterations of the original matrix equation for loop-tree and loop-star basis. Fig. 7 shows the number of iterations for a conducting plate. The plate is excited by a delta-gap source on the strip. The matrix equation based on loop-star basis is always divergent. The matrix equation based on loop-tree basis converges but with very large number of iterations. However, the transformed matrix equations have significantly reduced iteration counts. The plane wave excitation case gives almost the same results.

To prove the capability of the proposed method and its capability from very low frequencies to electrodynamic frequencies for complex structures, the input impedance of a Hertzian dipole is calculated. The so-called Hertzian dipole comprises two conducting spheres connected by a length of wire and fed at the center of the wire. We first use the loop-tree basis with basis rearrangement to improve the iteration convergence at very low frequencies and then switch over to the RWG basis when frequency is high. At very low frequencies, the Hertzian dipole resembles a series LC network. The input impedance is

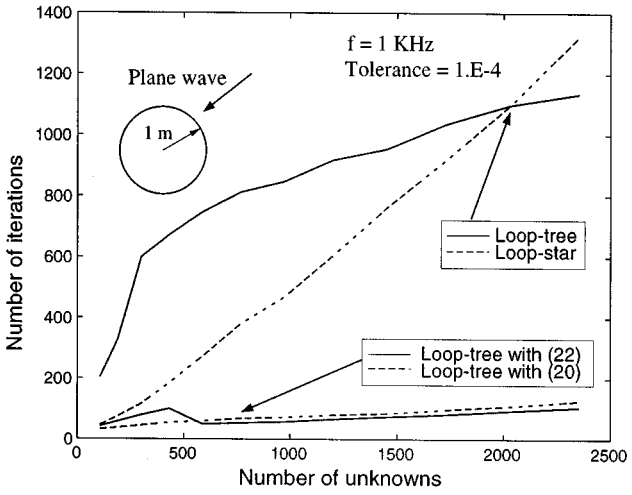


Fig. 6. Number of iterations versus the number of unknowns for different cases. The testing object is a conducting sphere whose radius is 1 m and is illuminated by a plane wave. The frequency is 1 KHz. The tolerance is $10^{-4}$. Diagonal preconditioning is applied to all cases.

$$Z_{\text{in}} = -i\omega L - \frac{1}{i\omega C} \tag{39}$$

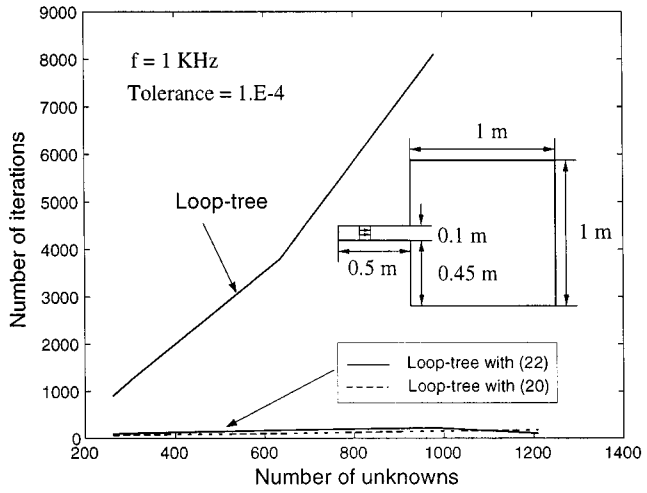


Fig. 7. Number of iterations versus the number of unknowns for different cases. The testing object is a conducting plate excited by a delta-gap source at the arm. The frequency is 1 kHz. The tolerance is $10^{-4}$. Diagonal preconditioning is applied to all cases.

where $L$ is the inductance and $C$ is the mutual capacitance between the two spheres. Because the inductance of the wire is very small, at very low frequencies, the input impedance is approximated by

$$Z_{\text{in}} \approx -\frac{1}{i\omega C}. \tag{40}$$

Fig. 8 shows the input impedance of the Hertzian dipole from 1 Hz to 100 MHz. Fig. 8(a) shows the comparison of the reactance from plain CG, LF-MLFMA and the capacitor approximation at very low frequencies. The loop-tree basis with basis rearrangement is used in the LF-MLFMA and the plain CG method. Fig. 8(b) shows the input resistance and reactance from about 10–100 MHz. We use loop-tree basis at frequencies near 10 MHz and then switch to the RWG basis. Only plain CG method is used in this frequency range. We observe that the EM physics is correctly captured by the solution method. At low frequencies, the Hertzian dipole correctly behaves like a capacitor, while at higher frequencies, it behaves like an LC tank circuit.

Fig. 9 shows the comparison of the input admittance of a wire antenna mounted on a conducting plate between the numerical results and the experimental results done by Chao *et al.* [51]. The agreement is very good. The time dependence is chosen as $e^{j\omega t}$ here to meet the convention in [51].

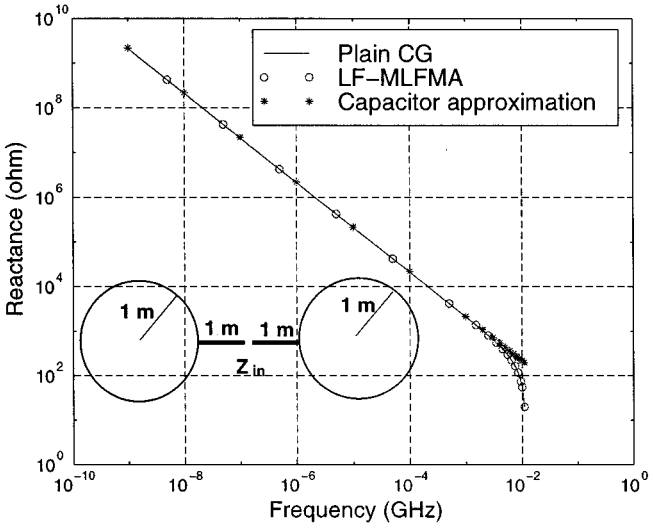


(a)

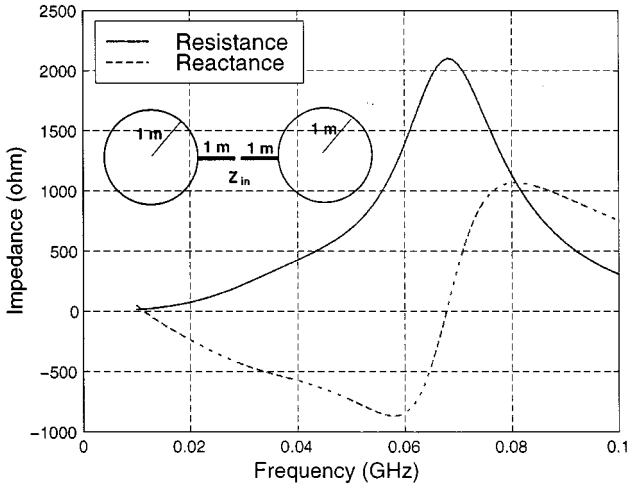


(b)

Fig. 8. Input impedance of a Hertzian dipole from very low frequency to microwave frequency. (a) Input reactance at very low frequencies. Rearranged loop-tree basis is used. (b) Input resistance and reactance from the plain CG method. Rearranged loop-tree and RWG bases are used separately at different frequencies.

## V. Conclusion

The matrix equations of EFIE at very low frequencies based on the loop-tree basis and the loop-star basis are transformed by a connection matrix, which represents a rearrangement of the basis. The new representation of the matrix equations can be solved efficiently by iterative solvers. It converges fast and no low-frequency break-down occurs in the numerical computation. A method to perform the multiplication of the inverses of the connection matrix and its transpose with a vector with only $O(N)$ floating-point operations is also developed. When the LF-MLFMA is applied to solve large-scale problems, the matrix transformation does not increase the computational complexity. The memory requirements and the number of floating-point operations still scale as $O(N)$ as in LF-MLFMA.

The matrix transformation here can also be viewed as a preconditioning procedure whereby the convergence and the spectral property of the original matrix has been changed by the matrix transformation. The important result here is that the application of this matrix transformation can be effected in $O(N)$ operations with a minimal cost. Therefore, this preconditioning procedure can be combined with the LF-MLFMA that performs a matrix–vector product in $O(N)$ operations, without increase the overall complexity of the solution method. This work has been incorporated into LF-MLFMA to solve large problems at very low frequencies. The LF-MLFMA can also be merged with the dynamic MLFMA to solve large-scale problems all the way from zero frequency to electrodynamic frequencies.

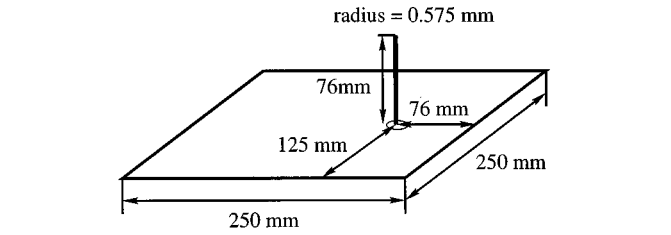


(a)

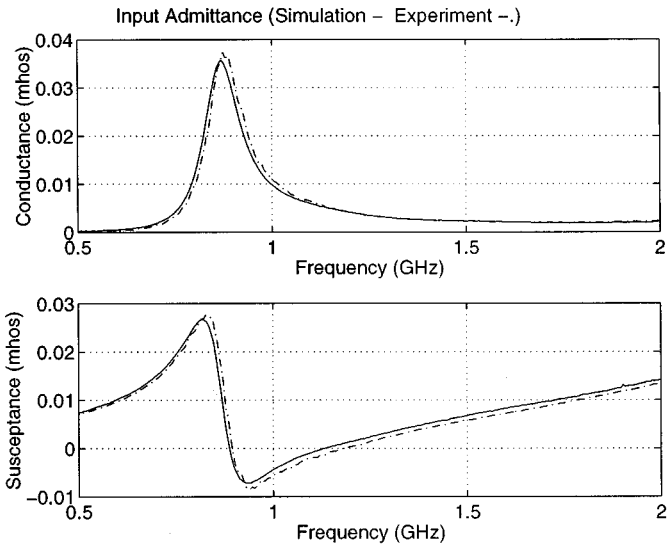


(b)

Fig. 9. Input admittance of a wire antenna mounted on a conducting plate. (a) Geometry of the wire antenna mounted on a conducting plate. (b) Comparison of the input admittance between numerical results and experimental results [51].

## ACKNOWLEDGMENT

This paper is dedicated to the memory of James R. Wait.

## REFERENCES

[1] J. C. Maxwell, *A Treatise on Electricity and Magnetism*. Oxford, U.K.: Clarendon, 1873.
[2] G. Mie, "Beiträge zur optik trüber medien speziel kolloidaler metallösungen," *Ann. Phys. (Leipzig)*, vol. 25, p. 377, 1908.
[3] P. Debye, *The Collected Papers of Peter J. W. Debye*. New York: Intersci., 1954.
[4] A. Sommerfeld, *Partial Differential Equation*. New York: Academic, 1949.
[5] N. Marcuvitz, "Field representations in spherically stratified regions," *Commun. Pure Appl. Math.*, vol. 4, pp. 263–315, 1951.
[6] J. R. Wait, "Scattering of plane wave from a circular dielectric cylinder at oblique incidence," *Can. J. Phys.*, vol. 33, no. 5, pp. 189–195, 1955.
[7] ——, "Radiation from a vertical antenna over a curved stratified ground," *J. Res. NBS*, vol. 56, p. 237, 1956.
[8] J. J. Bowman, T. B. A. Senior, and P. L. E. Uslenghi, *Electromagnetic and Acoustic Scattering by Simple Shapes*. Amsterdam, The Netherlands: North-Holland, 1969.
[9] M. Born and E. Wolf, *Principles of Optics*. New York: Pergamon, 1970.
[10] J. B. Keller, "Diffraction by a convex cylinder," *IRE Trans. Antennas Propagat.*, vol. AP-4, pp. 312–321, July 1956.
[11] S. W. Lee and G. A. Deschamps, "A uniform aymptotic theory of EM diffraction by a curved wedge," *IEEE Trans. Antennas Propagat.*, vol. AP-24, pp. 25–34, Jan. 1976.
[12] L. B. Felsen and N. Marcuvitz, *Radiation and Scattering of Electromagnetic Waves*. Englewood Cliffs, NJ: Prentice-Hall, 1973.
[13] P. H. Pathak, "An asymptotic analysis of the scattering of plane waves by a smooth convex cylinder," *Radio Sci.*, vol. 14, p. 419, 1979.
[14] R. G. Kouyoumjian, "The geometrical theory of diffraction and its applications," in *Numerical and Asymptotic Techniques in Electromagnetics*, R. Mittra, Ed. New York: Springer-Verlag, 1975.
[15] H. Bremmer, "The WKB approximation as the first term of a geometric-optical series," *Commun. Pure Appl. Math.*, vol. 4, p. 105, 1951.
[16] V. A. Fock, *Electromagnetic Diffraction and Propagation Problems*. New York: Pergamon, 1965.
[17] D. S. Jones and M. Kline, "Asymptotic expansion of multiple integrals and the method of stationary phase," *J. Math. Phys.*, vol. 37, pp. 1–28, 1958.
[18] W. C. Chew, *Waves and Fields in Inhomogeneous Media*. New York: Van Nostrand Reinhold, 1990.
[19] K. S. Yee, "Numerical solution of initial boundary value problems involving Maxwell's equations in isotropic media," *IEEE Trans. Antennas Propagat.*, vol. 14, pp. 302–307, May 1966.
[20] P. P. Silvester and R. L. Ferrari, *Finite Elements for Electrical Engineers*. Cambridge, U.K.: Cambridge Univ. Press, 1983.
[21] R. F. Harrington, *Field Computation by Moment Method*. Malabar, FL: Krieger, 1983.
[22] S. M. Rao, D. R. Wilton, and A. W. Glisson, "Electromagnetic scattering by surfaces of arbitrary shape," *IEEE Trans. Antennas Propagat.*, vol. AP-30, pp. 407–418, May 1982.
[23] J. M. Song, C. C. Lu, W. C. Chew, and S. W. Lee, "Fast Illinois solver code (FISC) solves problems of unprecedented size at the Center for Computational Electromagnetics, University of Illinois," *IEEE Antennas Propagat. Mag.*, vol. 40, pp. 27–34, June 1998.
[24] A. F. Peterson, "The 'interior resonance' problem associated with surface integral equations of electromagnetics: Numerical consequences and a survey of remedies," *Electromagn.*, no. 10, pp. 293–312, 1990.
[25] J. C. Bolomey and W. Tabbara, "Numerical aspects on coupling between complementary boundary value problems," *IEEE Trans. Antennas Propagat.*, vol. AP-21, pp. 356–363, May 1973.
[26] J. R. Mautz and R. F. Harrington, "H-field, E-field, and combined field solutions for conducting bodies of revolution," *AEÜ*, vol. 32, no. 4, pp. 159–164, Apr. 1978.
[27] H. A. Schenck, "Improved integral formulation for acoustic radiation problems," *J. Acoust. Soc. Amer.*, vol. 44, pp. 41–48, July 1968.
[28] P. C. Waterman, "Numerical solution of electromagnetic scattering problems," in *Computer Techniques for Electromagnetics*, R. Mittra, Ed. New York: Hemisphere, 1987.
[29] R. Mittra and C. A. Klein, "Stability and convergence of moment method solution," in *Numerical and Asymptotic Techniques in Electromagnetics*, R. Mittra, Ed. New York: Springer-Verlag, 1975.
[30] J. R. Mautz and R. F. Harrington, "A combined-source formulation for radiation and scattering from a perfectly conducting body," *IEEE Trans. Antennas Propagat.*, vol. AP-27, pp. 445–454, July 1979.
[31] A. R. Tobin, A. D. Yaghjian, and M. M. Bell, "Surface integral equations for multi-wavelength arbitrary shaped, perfectly conducting bodies," in *Proc. Dig. 19th URSI Radio Sci. Meet.*, Boulder, CO, Jan. 1987, p. 7.
[32] L. Greengard and V. Rokhlin, "A fast algorithm for particle simulation," *J. Computat. Phys.*, vol. 73, pp. 325–348, 1987.
[33] K. Nabor, S. Kim, and J. White, "Fast capacitance extraction of general three-dimensional structures," *IEEE Trans. Microwave Theory Tech.*, vol. 40, pp. 1496–1506, July 1992.
[34] V. Rokhlin, "Rapid solution of integral equations of scattering theory in two dimensions," *J. Comput. Phys.*, vol. 36, no. 2, pp. 414–439, 1990.
[35] W. C. Chew, J. M. Jin, C. C. Lu, E. Michielssen, and J. M. Song, "Fast solution methods in electromagnetics," *IEEE Trans. Antennas Propagat.*, vol. 45, pp. 533–543, Mar. 1997.
[36] J. R. Wait, *Geoelectromagnetism*. New York: Academic, 1982.
[37] D. R. Wilton and A. W. Glisson, "On improving the electric field integral equation at low frequencies," in *Proc. URSI Radio Sci. Meet. Dig.*, Los Angeles, CA, June 1981, p. 24.
[38] J. R. Mautz and R. F. Harrington, "An E-field solution for a conducting surface small or comparable to the wavelength," *IEEE Trans. Antennas Propagat.*, vol. 32, pp. 330–339, Apr. 1984.
[39] J. S. Lim, S. M. Rao, and D. R. Wilton, "A novel technique to calculate the electromagnetic scattering by surfaces of arbitrary shape," in *Proc. URSI Radio Sci. Meet. Dig.*, Ann Arbor, MI, June 1993, p. 322.
[40] W. Wu, A. W. Glisson, and D. Kajfez, "A comparison of two low-frequency formulations for the electric field integral equation," in *Proc. 10th Annu. Rev. Progress Appl. Computat. Electromagn.*, vol. 2, Monterey, CA, Mar. 1994, pp. 484–491.
[41] ——, "Electromagnetic scattering by resonant low-frequency structures," in *Proc. URSI Radio Sci. Meet. Dig.*, Seattle, WA, June 1994, p. 137.

[42] E. Arvas, R. F. Harrington, and J. R. Mautz, "Radiation and scattering from electrically small conducting bodies of arbitrary shape," *IEEE Trans. Antennas Propagat.*, vol. 34, pp. 66–77, Jan. 1986.
[43] M. Burton and S. Kashyap, "A study of a recent, moment-method algorithm that is accurate to very low frequencies," *Appl. Computat. Electromagn. Soc. J.*, vol. 10, no. 3, pp. 58–68, Nov. 1995.
[44] W. Wu, A. W. Glisson, and D. Kajfez, "A study of two numerical solution procedures for the electric field integral equation at low frequency," *Appl. Computat. Electromagn. Soc. J.*, vol. 10, no. 3, pp. 69–80, Nov. 1995.
[45] J. S. Zhao and W. C. Chew, "Three dimensional multilevel fast multipole algorithm from static to electrodynamic," *Microwave Opt. Tech. Lett.*, vol. 26, no. 1, pp. 43–48, July 2000.
[46] S. M. Rao, "Electromagnetic scattering and radiation of arbitrarily shaped surfaces by triangular patch modeling," Ph.D. dissertation, Univ. Mississippi, Oxford, MS, 1980.
[47] M. F. Costa and R. F. Harrington, "Electromagnetic radiation and scattering from a system of conducting bodies interconnected by wires," Syracuse Univ., Syracuse, NY, 1983.
[48] ——, "Minimization of the radiation from computer systems," in *Proc. Inst. Elect. Eng. Conf. Expo.*, Toronto, Canada, Sept. 1983, paper 83 261, pp. 660–665.
[49] F. Yuan, "Analysis of power/ground noise and decoupling capacitors in printed circuit board systems," in *Proc. IEEE Electromagn. Compat. Symp.*, Austin, TX, Aug. 1997, pp. 425–430.
[50] C. Lanczos, *Applied Analysis*. Englewood Cliffs, NJ: Prentice-Hall, 1956, pp. 141–143.
[51] H. Y. Chao, W. C. Chew, J. M. Song, and E. Michielssen, "Impedance calculation of complex surfaces-wire structures with the multilevel fast multipole algorithm and a variational formulation," in *IEEE Antennas Propagat. Soc. Int. Symp.*, Orlando, FL, July 1999.
[52] J. C. Maxwell, *A Treatise on Electricity and Magnetism*. New York: Dover, 1954.
[53] W. C. Chew, *Waves and Fields in Inhomogeneous Media*. New York: IEEE Press, 1995.

**Jun-Sheng Zhao** (M'98) was born in Shandong province, China, on April 17, 1966. He received the B.S. degree from Shandong University, China, in 1985, the M.E. degree from the Second Academy of the Ministry of the Astronautics Industry of China (now China Aerospace Industry Corporation), in 1988, and the Ph.D. degree from Tsinghua University, China, in 1995, all in electrical engineering.

From July 1988 to February 1992 and from July 1995 to January 1996, he worked at the Second Academy of the Ministry of the Astronautics Industry of China. From February 1996 to February 1999, he was a Visiting Postdoctoral Research Associate at the Center for Computational Electromagnetics, University of Illinois at Urbana-Champaign. From February 1999 to October 1999, he was a Postdoctoral Fellow at the Department of Electrical and Computer Engineering, Concordia University, Montreal, QC, Canada. Since November 1999, he has been a Research Scientist at the Center for Computational Electromagnetics, University of Illinois at Urbana-Champaign. His research interests include fast algorithms for computational electromagnetics, microwave integrated circuits, and ferrite devices.

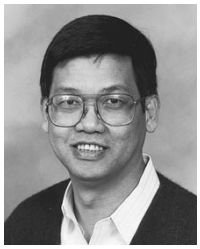

**Weng Cho Chew** (S'79–M'80–SM'86–F'93) was born on June 9, 1953 in Malaysia. He received the B.S. degree in 1976, both the M.S. and Eng. degrees in 1978, and the Ph.D. degree in 1980, all in electrical engineering from the Massachusetts Institute of Technology (MIT), Cambridge.

Previously, he has also analyzed electrochemical effects and dielectric properties of composite materials, microwave and optical waveguides, and microstrip antennas. From 1981 to 1985, he was with Schlumberger-Doll Research, Ridgefield, CT. While he was there, he was a Program Leader and later, a Department Manager. From 1985 to 1990, he was an Associate Professor with the University of Illinois. He is currently a Professor there and teaches graduate courses in waves and fields in inhomogeneous media, and theory of microwave and optical waveguides and supervises a graduate research program. He authored *Waves and Fields in Inhomogeneous Media* (New York: Van Nostrand Reinhold, 1990; New York: IEEE Press, 1995, 2nd printing), published over 200 scientific journal articles, and presented over 270 conference papers. He has been an Associate Editor of *Journal of Electromagnetic Waves and Applications* (1996–present), *Microwave Optical Technology Letters* (1996–present), the *International Journal of Imaging Systems and Technology* (1989–1994). He has been a Guest Editor of *Radio Science* (1986), *International Journal of Imaging Systems and Technology* (1989), and *Electromagnetics* (1995). From 1989 to 1993, he was the Associate Director of the Advanced Construction Technology Center, University of Illinois. Presently, he is the Director of the Center for Computational Electromagnetics and the Electromagnetics Laboratory at the same university. His recent research interest has been in the area of wave propagation, scattering, inverse scattering, and fast algorithms related to scattering, inhomogeneous media for geophysical subsurface sensing and nondestructive testing applications.

Dr. Chew is a member of Eta Kappa Nu, Tau Beta Pi, URSI Commisions B and F, and an active Member with the Society of Exploration Geophysics. He was an National Science Foundation Presidential Young Investigator for 1986. He was also an AdCom Member IEEE Geoscience and Remote Sensing Society. His name is listed many times in the *List of Excellent Instructors* on campus. He is an Associate Editor of the IEEE TRANSACTIONS OF GEOSIENCE AND REMOTE SENSING (1984–present), Recently, he has been selected to receive the 2000 IEEE Graduate Teaching Award. He is a Founding Professor of Engineering, University of Illinois.